TECHNICAL UNIVERSITY OF CLUJ-NAPOCA

ACTA TECHNICA NAPOCENSIS

Series: Applied Mathematics, Mechanics, and Engineering
Vol. 65, Issue II, June, 2022

MAGNETIC FIELD SIMULATION OF THREE-CORE SUBMARINE POWER CABLE

Wafa KRIKA, Ahmed Nour El Islam AYAD, Abdelghani AYAD

Abstract: *Several researches have been conducted on the electromagnetic effect in submarine power cables due to the magnetic interaction of the power lines on materials and environment. Our work aims to study the two-dimensional numerical simulation by using the finite element method of a three-core submarine power cable. The simulation findings illustrate the magnetic field in normal and abnormal conditions: under overload and different waveforms of current faults as functions of time and distance, in three phases. The results expose the magnetic field emission of high voltage submarine electric cable, distribution, waveform and intensities around and near the subsea cable.*

Key words: *Electric power cable, emission, fault, magnetic field, submarine.*

1. INTRODUCTION

Over the past two decades, submarine power cables were widely used with important growth, significantly in wind farms and energy transmission between countries, within the distribution and electrical transmission networks [1-3]. However, the submarine cable has short and long-term impacts on the environment such as: biological changes, chemical pollution, underwater noise and electromagnetic field emissions, heat emissions,...etc. [2,3]. The high voltage submarine lines at a long distance generate an important magnetic field near and around the electric cable [3-6].

Many researchers have studied the electromagnetic field characteristics, the interference, the effect of power and the type of current HVDC or HVAC (direct or alternating current) [7-12]. Other studies have developed models for computing electric field, emitted by subsea lines of HV and MV of monopolar, bipolar and three-phase cables systems, to detect structural isolation default of material by partial discharge (using analytical or numerical calculations) [13-15]. Other research has shown the magnetic effect by varying many parameters like the cable type: the distance between conductors, the resistivity of sol, harmonics and balanced load between the three phases in the power transmission line [16-20]. On the other hand, there were a few studies on the magnetic effect with electric fault variation of extra-high voltage cable (EHV) depending on time variation [21,22]. The presence of current defects has a big influence on the stability and reliability of power networks and cable insulation. It affects the quality and the continuity of energy network services [23-26].

The electric cable defect is divided into external or internal aggression (lightning overvoltage, circuit breaker switching operation or transient fault, short circuit). The line parameters change causes transmission of electromagnetic energy within the grid created by the augmentation of voltage and current.

The space in manufacturers' cable catalogs is usually reserved only in the normal conditions with industrial frequency (50 or 60 Hz). The knowledge of the magnetic field value at several levels and abnormal states is a major preoccupation for researchers. This paper studies the magnetic behavior with current fault, characterized by different values of frequency and amplitude in a three-core lead sheathed XLPE HVAC (cross-linked polyethylene, high-

Received: 30.04.22; **Similarities**: 18.05.22: **Reviewed**: 11.06./07.06.22: **Accepted**:20.06.22.

voltage alternating current) submarine cable (500 mm², 220 kV). The simulation results of marine electrical cable presented by COMSOL multiphysics, with Matlab software show the magnetic field density distribution. Around three core cables in normal condition, and in cases of the presence of: overload, switching short circuit current at temporary study in three-phase. Therefore, it is necessary to study the magnetic characteristics in the steady and abnormal state: near field, (two points N and F characterized by shorter or greater distances from the source) of the subsea cable.

2. THREE CORE SUBMARINE CABLE

HVAC submarine cables were developed to carry a great amount of power across the water. The cable conductors consist of copper or aluminum, depending on size and price. Cross-linked polyethylene (XLPE), with a maximum operating temperature of 90°C, is a commonly used insulation material [27]. A common construction of a three-core XLPE separate lead sheath-type submarine cable is shown in fig.1 with frequency 50 Hz, Rated current (Amplitude) $926 \cdot \sqrt{2}$ A , Phase to ground voltage $220/\sqrt{3}$kV where it contains:

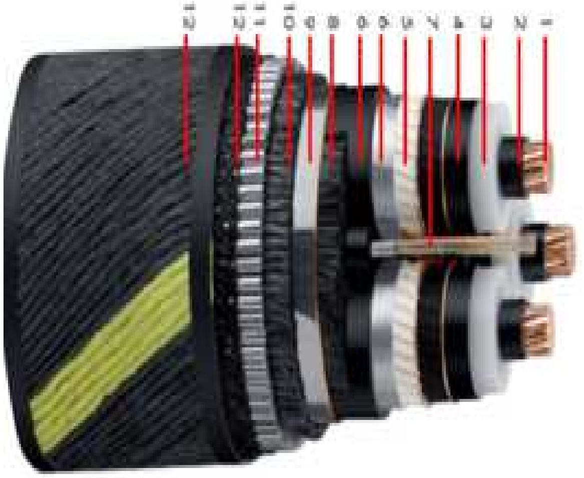

1: Conductor 2: Conductor screen, 3:Insulation, 4:Insulation screening-semi conductive, 5:Screen, 6:Laminated sheath, 7:Optical fibers-optically used for telecommunications, 8:Fillers, 9: Binder tapes 10:Armour Bedding-polypropylene strings, 11: Armor-galvanized round steel wires, 12:Serving.

Fig. 1. Three core cable shape [27]

2.1 Materials Data

Table 1 gives the structure sizes and characteristics of cable. Table 2 presents the characteristics of different materials used in the model simulation, for both single-core and three-core submarine electrical cables.

Table 1: Structure size of three core XLPE cable

Description	**Value [mm]**
Diameter of the conductor (Phase)	26.2
Insulation thickness (Phase)	24
Semi-conductive compound thickness (Phase)	0.85
Lead sheath thickness (Phase)	2.9
Diameter of fiber optic cable core	2.5
Armor thickness	6.5
Outer diameter of the cable	219
Diameter over insulation (Phase)	77.6
Diameter over phase (Phase)	89.2
Diameter over fiber optic core	2.5

Table 2 . Materials characteristics of submarine power cables [27,28].

Materials	**Electrical conductivity [S/m]**	**Relative permeability (per unit)**	**Relative permittivity (per unit)**
Air	$1 \cdot 10^{-14}$	1	1
Polyethylene	$1 \cdot 10^{-18}$	1	2.25
Polypropylene	$1 \cdot 10^{-18}$	1	2.36
XLPE	$1 \cdot 10^{-18}$	1	2.5
Lead	$4.55 \cdot 10^{6}$	1	1
Copper	$5.998 \cdot 10^{7}$	1	1
High-strength alloy steel	$4.032 \cdot 10^{6}$	1	1
Semi-conductive compound	2	1	1
Silica glass	$1 \cdot 10^{-14}$	1	2.09
Sandy	1	1	28
Water	$5.5 \cdot 10^{-6}$	1	81

2.2 Calculation of the Magnetic Field:

The magnetic submarine cable study aims to show the field lines distribution and magnitude at several positions. In theory, the resolution of the simulation model using differential or integrative equations is depending on the condition and the properties of the problem of device, solved by Maxwell's equations [21,28,29].

A- Maxwell's equation in variable regime:

The four partials differentials Maxwell's equations explain the behavior of electromagnetic fields in the form of a mathematical model that employs proportional relationships related to the properties of materials and media, known by constitutive relations. The following equations represent Maxwell's law [21,28,30]:

$$\nabla \cdot D = \rho \qquad (1)$$

$$\nabla \times E = -\frac{\partial B}{\partial t} \qquad (2)$$

$$\nabla \cdot B = 0 \qquad (3)$$

$$\nabla \times H = J' = J + J_D \qquad (4)$$

Where:
$\vec{D}$: The electric induction or electric displacement vector. : the electric charge density $\vec{E}$: the electric field vector $\vec{B}$: the magnetic induction vector $\vec{H}$: the Magnetic field vector $\vec{J'}$: the electric current density $\vec{J}$: the conduction current density $\overrightarrow{J_D} = \frac{\partial \vec{D}}{\partial t}$: the displacement current density [21]. The constitutive equation given the relations between the fields by physical property in the subdomain:

$$B = \mu H = \mu_0 \mu_r H \qquad (5)$$

$$J = \sigma E \qquad (6)$$

Where: μ, μ_0, μ_r : Permeability of the medium, vacuum, and relative respectively, σ Electrical conductivity [21,30].

B- Numerical Model:

The model solves Maxwell-Ampère's law in 2D, using the out-of-plane magnetic vector potential A as a dependent variable [28]. All Maxwell's equations are either directly or indirectly involved together with three constitutive relations and applied the mathematical operation for establishing the final equation problem. We start with the combination of Gauss's and current conservation law. In the frequency domain this gives:

$$\nabla \cdot (\boldsymbol{J} + j\omega \boldsymbol{D}) = 0 \qquad (7)$$

When we replace the constitutive relations, we get the following equation:

$$\nabla \cdot (\sigma \boldsymbol{E} + j\omega\varepsilon \boldsymbol{E}) = 0 \qquad (8)$$

The current density is defined by; $\boldsymbol{J}' = \boldsymbol{J} + j\omega \boldsymbol{D}$ is the sum of both conduction current and displacement current [21,28].

The second step of the model starts with Maxwell-Ampere's law; $\nabla \times \boldsymbol{H} = \boldsymbol{J}'$ then takes the divergence of that to get:

$$\nabla \cdot (\nabla \times \boldsymbol{H}) = \nabla \cdot \boldsymbol{J}' = \nabla \cdot (\boldsymbol{J} + j\omega \boldsymbol{D}) = 0 \qquad (9)$$

We add the magnetic constitutive relation; $B = \mu H$

$$(\nabla \times \boldsymbol{H}) = (\nabla \times (\boldsymbol{\mu}^{-1} \boldsymbol{B})) = \boldsymbol{J}' = (\sigma + j\omega\varepsilon) \boldsymbol{E} \qquad (10)$$

Next, let consider the concept of a vector field A, the magnetic vector potential that is

$$\nabla \times \boldsymbol{A} = \boldsymbol{B} \qquad (11)$$

And take the divergence

$$\nabla \cdot (\nabla \times \boldsymbol{A}) = \nabla \cdot \boldsymbol{B} = 0 \qquad (12)$$

Maxwell's Faraday equation used for expressed E in terms of A [21,28].

$$\nabla \times \boldsymbol{E} = -j\omega \boldsymbol{B} \qquad (13)$$

$$\nabla \times \boldsymbol{E} = -j\omega(\nabla \times \boldsymbol{A}) = \nabla \times (-j\omega \boldsymbol{A}) \qquad (14)$$

$$\boldsymbol{E} = -j\omega \boldsymbol{A} \qquad (15)$$

Now, both B and E expressed in terms of A, if we substitute this result in (11) we will find:

$$\nabla \times (\boldsymbol{\mu}^{-1} \nabla \times \boldsymbol{A}) = (\sigma + j\omega\varepsilon)(-j\omega \boldsymbol{A}) \qquad (16)$$

Finally, if we swap about some terms and put everything on the left side, we get the following 2D partial differential equation for the dependent variable A:

Received: 30.04.22; **Similarities**: 18.05.22: **Reviewed**: 11.06./07.06.22: **Accepted**:20.06.22.

$$\nabla \times (\mu^{-1} \nabla \times A) - \omega^2 \varepsilon A + j\omega A = J_s \tag{17}$$

The magnetic fields interface uses this equation in the domains to determine the value of A and consequently, the value of all fields derived from it [21,28]. The input electric current of the three phases in time variation is as the following equations:

$$I_a = I_0, I_b = I_0 e^{\frac{-j2\pi}{3}}, I_c = I_0 e^{\frac{j2\pi}{3}} \tag{18}$$

C- Model presentation

The geometries model of the submarine power cables are represented by a graphic interface of the COMSOL multiphysics software. The cable placed in sand and the upper part at water (Fig. 2).

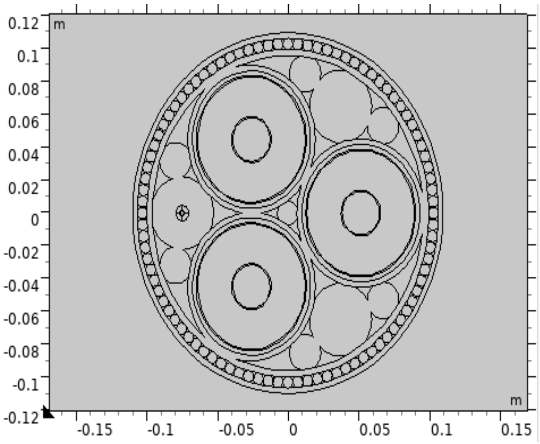

a-Three core cable model

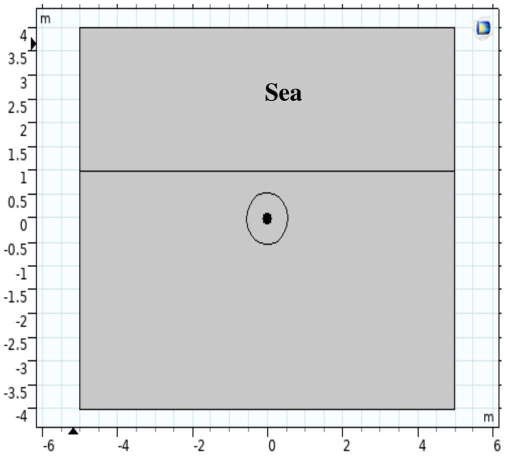

b-Submarine cable environment

Fig. 2. submarine power cable

D- Mesh Of Submarine Power Cables

Fig. 3 shows the mesh model of the submarine power cable by the finite element method. The discretization contains several nodes, triangles and elements, which depend on the studied system, the modeling was carried out in two dimensions axis [28,31,32].

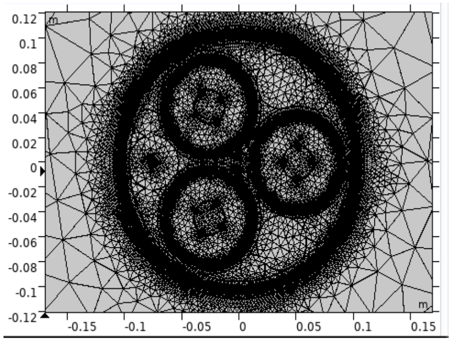

Fig. 3. Mesh of submarine three core electrical cable

3. SIMULATION RESULTS

Fig. 4 illustrates the magnetic flux density distribution of subsea three-core cable around the power line, placed at 1 m under the ground.

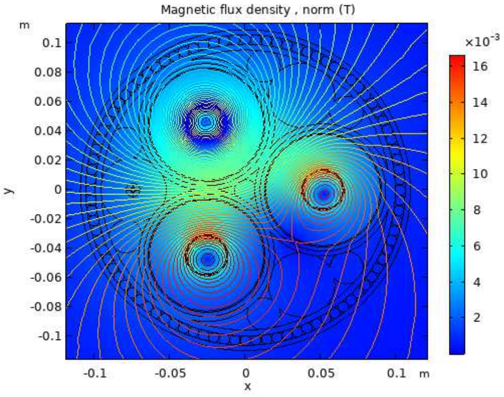

A-Three core cable

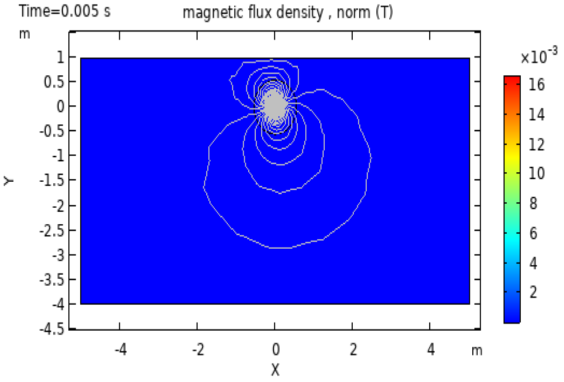

B- Magnetic field lines distribution

Fig. 4. Magnetic flux density in the frequency domain

The magnetic field peak value obtained is nearly above the lateral conductors. The important electrical current passed in the conductor, produces a significant magnetic flux density around the cable surface. The density passes across the different cable-layers to the outside. However, this concentration decreases as one move away from underground cables.

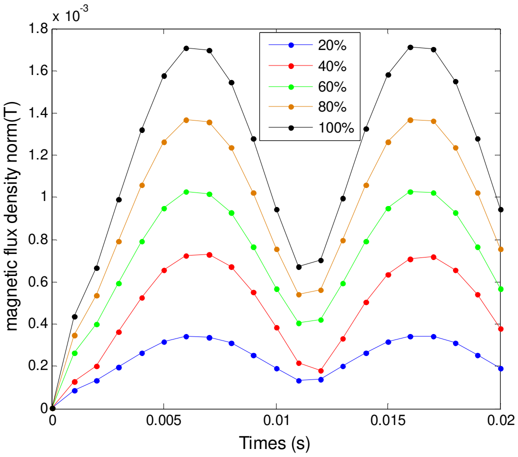

A- magnetic flux density with load and time variations

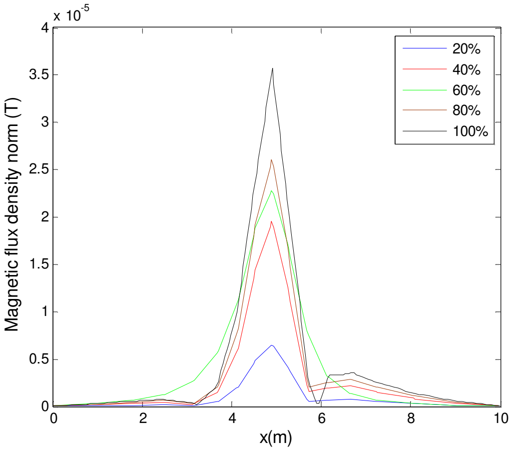

B- magnetic flux density with load and distance variations

Fig. 5. Magnetic field variation with distance, time, and load.

Fig. 5-A shows the magnetic flux density with load and time influence, in the extremity of the subsea cable (repetitive periodic signal in steady-state in normal condition).

Fig. 5-B represents the magnetic flux density amplitude as a function of distance with load variation, between sol and sea level (the maximum density is above the cable position with load of 100%). When the overcurrent passes a submarine electric conductor, it generates an important magnetic field, excessive heat, and risk of damage to equipment and cable isolation. The most rampant major causes of subsea power cable failures according to various studies are:

- Fishing activities, Electrical faults, Thermal effects, Environmental factors, ambient issues
- Mechanical faults, manufacturing errors, Ageing, Unknown causes, Poor installation [36-40].

The main important electrical faults (incidents) occurring in subsea power is: overvoltage, overloads, oscillations (switching inductive or capacitive loads), short circuit. Electrical faults consequences are: breakdown of the dielectric insulating, loss of power supply, the destruction of network elements, overheating of active parts, a strong power signal, the unbalance [37-44].

3.1 Current Fault Waveform Variation In Three-Core Submarine Cable

In the electrical network the presence of fault (Internal or external) characterized by frequencies and magnitude variations, results the several shapes in the time domain [33-35]. The following study shows the influence of the current waveforms faults produced by substation or network (breaker overcurrent short circuit or maximum load) on the generated magnetic field near the three-core cable. We studied the four cases:

A- Current without fault (steady-state, normal) C-Fault switching of I=1700 A with 2000 HZ. [36-44].
B- Overload rating of 120% of current, I=1111.2 A. D-Short circuit characterized by current of I=60 kA and 5 kHz

The simulation results show the magnetic flux with time variation in the water surface layer

Received: 30.04.22; **Similarities**: 18.05.22: **Reviewed**: 11.06./07.06.22: **Accepted**:20.06.22.

(the colors represent the different times in one period). The magnetic field amplitude has a proportional relation with the fault nature (three cases B, C, D) compared with case A without fault.

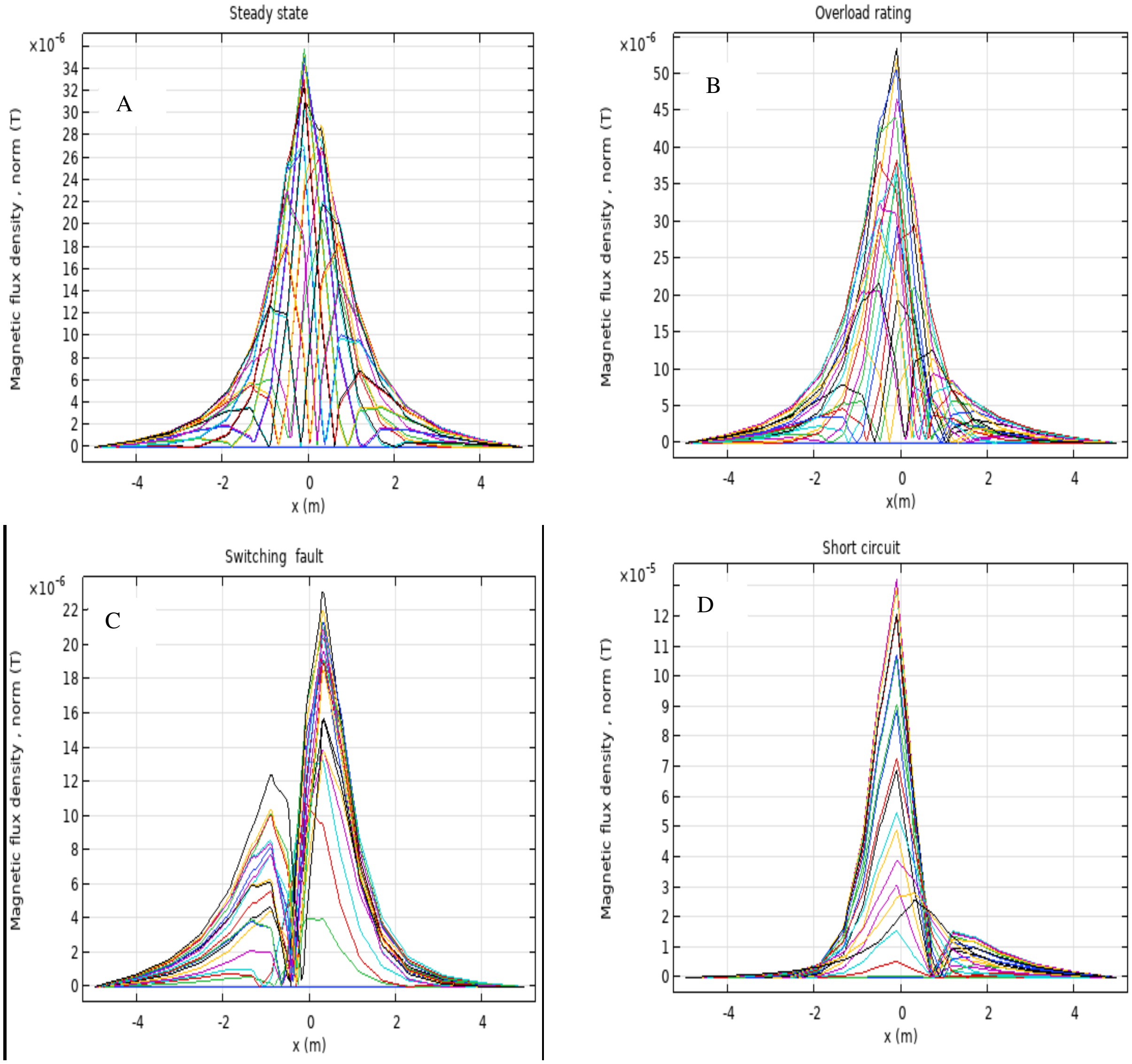

Fig. 6. magnetic flux density in the water surface

Fig. 6 shows the magnetic field lines spread near the submarine electric three-core cable in four cases. It can be seen that the magnetic field peak value is obtained nearly above the conductor center. The difference in level reached between case B and case A (50 and 34mT respectively) in low frequency with 20% because of the overload current (966 A and 1111.12A).

Then, these levels start to reduce gradually with the increase of lateral distance from the conductors. From these computations, we can see a significant variation of the graphs in transient cases (switching and short circuit) affected by the important applied fault currents magnitude and frequency (follow “equation (20),”). The difference of magnetic density level reached between case D and case C with 50 times more, because of the strong short circuit current, while the maximum current is greater than 35 times. This multiplication is explained by the effect of magnetic proximity between the three phases (the mutual inductive and capacitive effect between the different parts of the cable), the meaning of the multiple color curves (at different times). However, the two diagrams are not symmetrical because of the different phase shift delay.

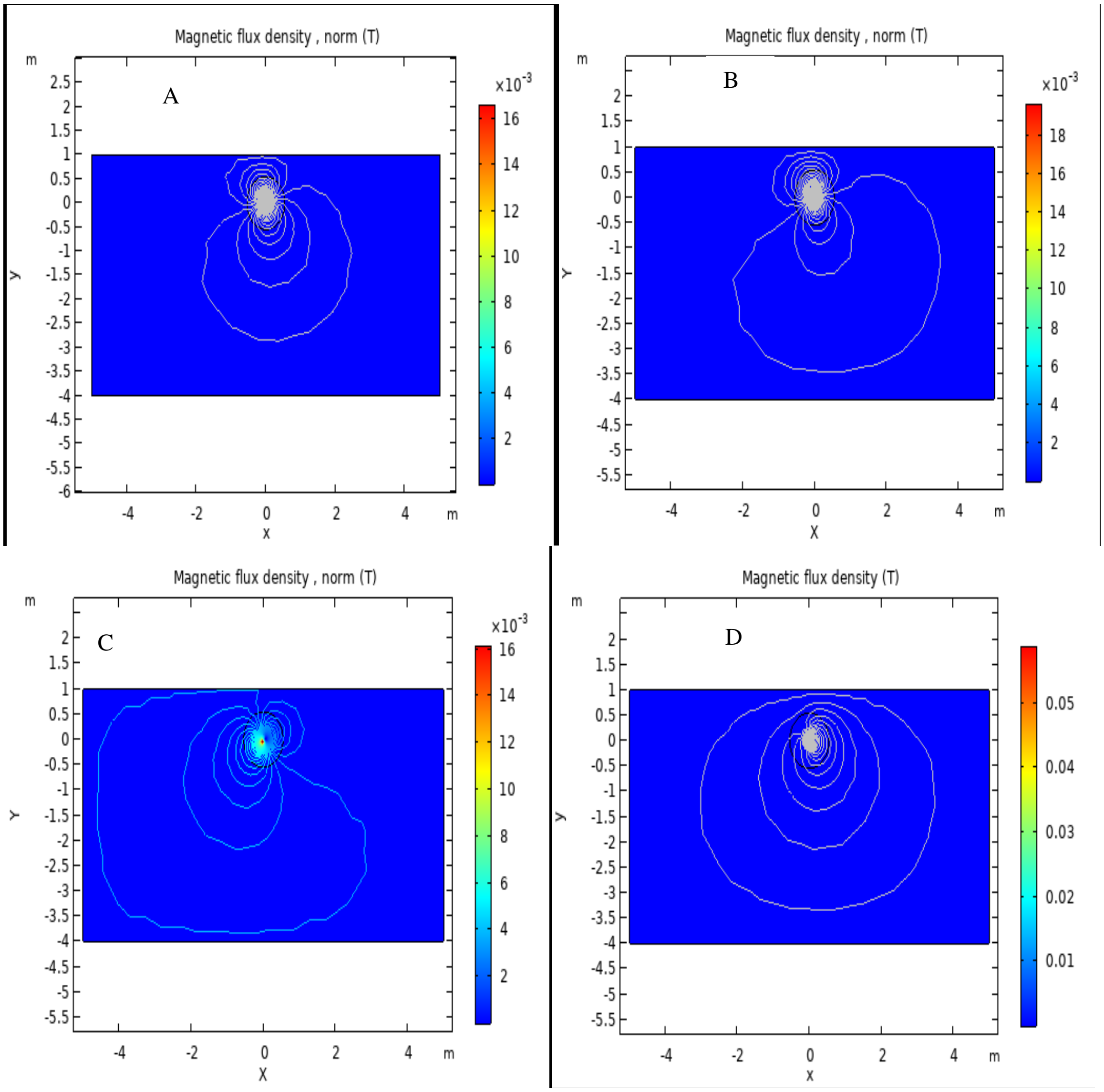

Fig. 7. Magnetic field lines propagation near the three-core submarine cable

Fig. 7 shows that the field lines spread strength are more widely according to the characteristics of the fault currents, compared to the normal case. The maximum value of magnetic flux density strength represented by contours is (e.g. 16, 20mT for steady-state and overload, but for switching is 16, and 50mT for short circuit). The strongest distribution line level of the magnetic field produced close to the subsea cable surface. The current fault waveform and magnitude have a significant effect on the magnetic flux density distribution and magnitude around the submarine conductors in the XY plane.

3.2 Symmetric Fault In Three-Core Submarine Cable

The calculation of magnetic flux density variation done in two points near the submarine

Received: 30.04.22; **Similarities**: 18.05.22: **Reviewed**: 11.06./07.06.22: **Accepted**:20.06.22.

power cable: N in the extremity of cable and F in the circle around the cables, which are characterized by shorter and greater distances from the magnetic source, in normal and fault condition (normal, abnormal condition of: A, B, C, D cases). See Fig. 8 and Fig. 9. We propose the symmetrical current variation in the three-phase of submarine power cable.

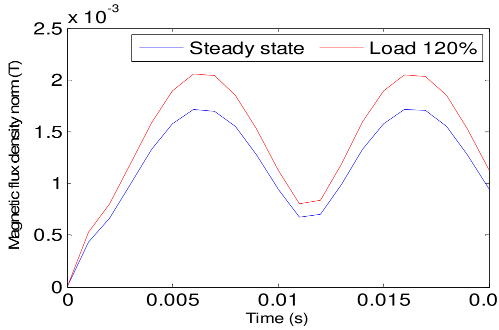

A- frequency 50Hz

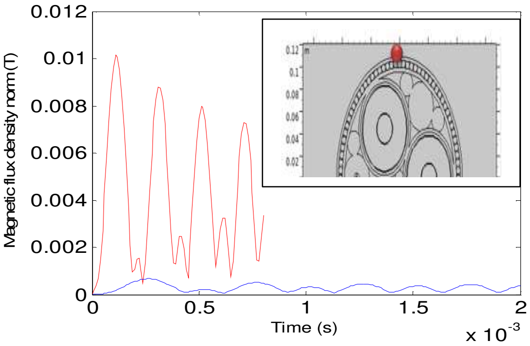

B- Transient state

Fig. 8. Temporary variation of magnetic flux near the cable extremity

The magnetic flux curve of the point near the three-core cable is characterized by an important variation with different waveforms (curve shape and maximum value) compared to the normal case. This change is due to the nature (waveform or shape, frequency, magnitude of fault) of the cable's current, where the maximum value is close to 2,1mT for overload, and 1.6mT in steady-state. For the transient state, the values are 2.5mT and 12mT for switching and short circuit respectively (Fig 8). The magnetic field calculation in far points of the three-core cable is given in Fig.9.

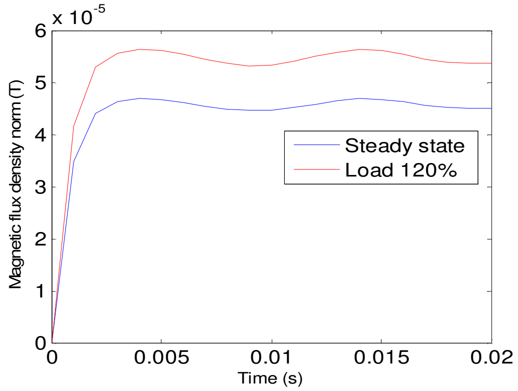

A- Frequency 50Hz

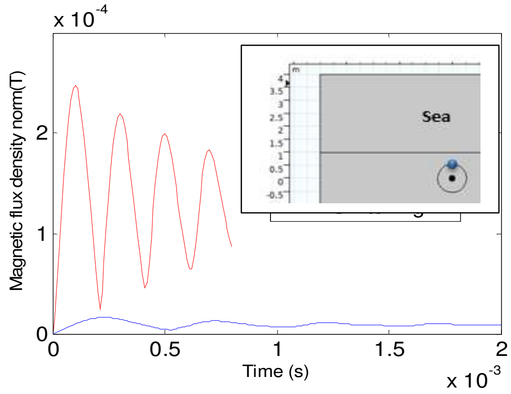

B- Transient state

Fig. 9. Temporary variation of magnetic flux far the cable

The simulation results show the important variation of magnetic flux density in the far point of three-core submarine power cable, in abnormal and transient conditions. The peak of the curve reaches a value of 0,2 mT for short circuit case compared to the first steady-state case (the reference) . The simulation proves that the magnetic flux density decreases in function of distance compared between Fig. 8 and 9. The magnetic field waveform variation and deformation are caUused by the electric current and mutual effect between three-phase fields.

4. CONCLUSION

In this paper, we presented the finite element analysis of magnetic fields emitted by submarine high-voltage power cables, using COMSOL Multiphysics 5.4 and Matlab software.

According to the simulation results, it can be drawn that the magnetic field lines have a greater concentration near the three-core submarine power cable, mainly with large electrical faults, but a decrease in function of far distance. It can be also observed that the magnetic flux density increases when the overcurrent fault is present as well as, the mutual coupling between defect phases. The overcurrent may lead to negative consequences such as excessive heating, damage to the insulation coordination, or the cable exit out of service. From this investigation, it is noticed that the obtained numerical model has the advantage to compute the magnetic flux density of the system with different values of current. This capacity allows deducing the magnetic field.

Future work will be focused on the simulation and measure of heat effects on submarine single and three core cables in normal and abnormal or transient conditions.

5. ACKNOWLEDGMENT

The authors are thankful to Hassiba Benbouali University of Chlef, and Kasdi Merbah University of Ouargla, Algeria, faculty of technology for providing necessary facilities and support and the General Directorate of Algerian Scientific Research (DGRSDT), under the project on RTR, Inductics-net.

6. REFERENCES

[1] G. Pedrazzoli and G. Rinzo, “HVAC Cable Systems,” *2018 IEEE International Conference on Environment and Electrical Engineering and 2018 IEEE Industrial and Commercial Power Systems Europe (EEEIC / I&CPS Europe)*, Palermo., Italy, 2018, pp. 1-6.

[2] B. Taormina et al., “A review of potential impacts of submarine power cables on the marine environment: Knowledge gaps, recommendations and future directions,” Renewable and Sustainable Energy Reviews, vol. 96, no. 7, pp. 380-391, July 2018.

[3] I. Jurdana, R. Ivče and D. Glažar, “Submarine optical cables: Impact on the marine environment," *Proceedings ELMAR-2014*, Zadar, Croatia, 2014, pp. 1-4.

[4] Meriouma, T., Bessedik, S.A., Djekidel, R. (2021). Modelling of electric and magnetic field induction under overhead power line using improved simulation techniques. European Journal of Electrical Engineering, Vol. 23, No. 4, pp. 289-300. https://doi.org/10.18280/ejee.230402

[5] W. Rijkswaterstaat, V. Leefomgeving , “Potential effects of electromagnetic fields in the Dutch North Sea Phase 1 – Desk Study Final report number: 16-101 2016 Case number: 31119002 WaterProof BV reference: WP2016_1031 Bureau Waardenburg report.

[6] Y. Guo et al., “The Review of Electromagnetic Pollution in High voltage Power Systems,” 3rd International Conference on Biomedical Engineering and Informatics (IEEE BMEI 2010), Yantai, China, 2010, pp 1322-1326.

[7] S. Vaideki et al., “ field analysis of high voltage submarine cables," *2017 International Conference on Computation of Power, Energy Information and Commuincation (ICCPEIC)*, Melmaruvathur, India, 2017, pp. 778-782.

[8] K. Jayasinghe, “ Power loss evaluation of submarine cables in 500mw offshore wind farm master of science," Ph.D. dissertation, department of earth sciences , uppsala university, Campus Gotland 2017.

[9] A. Pagnetti, “Cable modelling for electromagnetic transients in power systems," Ph.D. dissertation,University Blaise Pascal - Clermont-Ferrand II, 2012.

Received: 30.04.22; **Similaritie**s: 18.05.22: **Reviewed**: 11.06./07.06.22: **Accepted**:20.06.22.

[10] D. Elliott, et al., " A comparison of AC and HVDC options for the connection of offshore wind generation in Great Britain," IEEE Transactions on Power Delivery, Vol. 31, no. 2, pp. 798-809, April 2016.

[11] W. Mei et al., "Research and design of DC500kV optical fiber composite submarine cable," *2017 4th IEEE International Conference on Engineering Technologies and Applied Sciences (ICETAS)*, Salmabad, Bahrain, 2017, pp. 1-6.

[12] S. Tian, et al., "Simulating calculations of transient voltages and insulation coordination on 500 kV AC XLPE submarine cable line," *2017 International Conference on High Voltage Engineering and Power Systems (ICHVEPS)*, Denpasar, Indonesia, 2017, pp. 484-487.

[13] F. Dinmohammadi , et al., " Predicting Damage and Life Expectancy of Subsea Power Cables in Offshore Renewable Energy Applications ," IEEE Access, *Vol. 7, no. 1, pp. 54658-54669, May 2019.*

[14] M. Liu and C. Teng, "A multi-domain fault localization model for submarine cable system," *2011 13th Asia-Pacific Network Operations and Management Symposium*, Taipei, Taiwan, 2011, pp. 1-4.

[15] J. Kojima, "Optimization of pulse width for electric time domain reflectometry for fault point localization of power feeding lines of optical submarine cables," *2011 IEEE Symposium on Underwater Technology and Workshop on Scientific Use of Submarine Cables and Related Technologies*, Tokyo, Japan, 2011, pp. 1-4.

[16] M. A. Hamdan, J. A. Pilgrim and P. L. Lewin, "Effect of Sheath Plastic Deformation on Electric Field in Three Core Submarine Cables," *2018 IEEE Conference on Electrical Insulation and Dielectric Phenomena (CEIDP)*, Cancun, Mexico, 2018, pp. 342-345.

[17] A. Hafner, et al., "Impedance and Admittance Calculations of a Three-Core Power Cable by the Finite Element Method," International Conference on Power Systems Transients, Cavtat, Croatia, June 15-18, 2015.

[18] T. Ruixiang et al., "Calculation of Capacitance Parameters of XLPE Submarine Cable Based on Finite Element Method," *2019 IEEE 3rd International Conference on Circuits, Systems and Devices (ICCSD)*, Chengdu, China, 2019, pp. 45-49.

[19] C. H. Chien , " On the Steady-State Harmonic Performance of Subsea Power Cables Used in Offshore Power Generation Schemes ," Ph.D. dissertation, Mechanical Engineering University, College London, June 2007.

[20] I. M. de Alegria et al., "Transmission alternatives for offshore electrical power," Renewable and Sustainab, Pagele Energy Reviews, vol. 13,no. 5, pp. 1027–1038, June 2009.

[21] I. Benchebiba, O. Makhloufi , " Simulation of high voltage submarine power cables," master thesis, Kasdi merbah university of Ouargla, Algeria 2020.

[22] B. Zhu et al., "Study on On-line Insulation Monitoring for 500kV Submarine Cable," IEEE Workshop on Advanced Research and Technology in Industry Applications 2014 (WARTIA), Ottawa, ON, Canada,2014.

[23] M. T. Arentsen et al., " MVAC submarine cable, magnetic fields measurements and analysis," *2017 52nd International Universities Power Engineering Conference (UPEC)*, Heraklion, Greece, 2017, pp. 1-6.

[24] L. Zhang et al., “Study on Submarine Cable Overvoltage Impact Test Suppression Measures," IEEE International Power Electronics and Application Conference and Exposition, Shenzhen, China, 2018.

[25] S. Christou , “Thermal prognostic condition monitoring for mv cable systems," Ph.D. dissertation, faculty of Physical Sciences and Engineering, University of Southampton, June 2016.

[26] Y. G. sahin and F. Aras, “Investigation of harmonic effects on underground power cables”, 2007 International Conference on Power Engineering, Energy and Electrical Drives, Setubal, Portugal, April 12-14, 2007·

[27] Three-core submarine cable with aluminiumpolyethylene-laminated (APL) sheath Dreileiterseekabel, supplementary materials technical catalogue 2014 .www.nkt.com

[28] Theory for the Magnetic Fields,(2012) No Currents Interface User´s Guide magnetostatic equation AC/DC Module May Multiphysics software COMSOL 4.32012 www.comsol.com/support /releasenotes/4.2/acdc.

[29] F. Rachidi, "Formulation of the field-to-transmission line coupling equations in terms of magnetic excitation field," in *IEEE Transactions on Electromagnetic Compatibility*, vol. 35, no. 3, pp. 404-407, Aug. 1993, doi: 10.1109/15.277316.

[30] A. N. E. I. Ayad, W. Krika, H. Boudjella, A. Horch, Simulation of the electromagnetic field in the vicinity of the overhead power transmission line, European journal of Electrical Engineering, vol. 21, no. 1, pp. 49-53, 2019, doi: 10.18280/ejee.210108.

[31] Meunier G, The Finite Element Method, “ Theory, Implementation, and Applications’’ Book 2013, 395 edition hardcover Wiley.

[32] Djekidel, R., & Bessedik, S.-A. (2020) , " ASA Algorithm Combined with Current Simulation Method (CSM) for the Magnetic Induction under HV Power Lines in 3D Analysis Model," Advanced Electromagnetics, vol. 9, no. 2, pp. 7-18, 2019, doi https://doi.org/10.7716/aem.v9i2.1345.

[33] W. Krika , A.N.E Ayad , L. Benyekhlef, F. Benhamida, " Electromagnetic simulation of subsea power cable pollution, " International black sea coastline countries scientific research symposium VI, Giresun, Turkey , April 2021.

[34] W. Krika , A.N.E Ayad , L. Benyekhlef, F. Benhamida "Thermal effect of harmonic and short circuit in underground electric cable, " International black sea coastline countries scientific research symposium VI, Giresun, Turkey , April 2021.

[35] W. Krika , A.N.E Ayad , L. Benyekhlef, F. Benhamida "Electromagnetic simulation of underground power cable perforation by nail," International black sea coastline countries scientific research symposium VI, Giresun, Turkey , April 2021.

[36] H. ZHANG et al., "Study on Application Status of XLPE Insulated Submarine Cable Used in Offshore Wind Farm of China, " The Journal of Engineering The 6th International Conference on Renewable Power Generation (RPG) J.Eng, Vol. 2017, no. 13, pp. 702–707, 2017, doi:10.1049/joe.2017.0421.

[37] O. El Mountassir C.Strang-Moran Offshore Wind Subsea Power Cables Installation, Operation and Market Trends university of HULL technical rapport September 2018 AP-0018.

[38] F. Palone et al., "transients on very long HV ac cable lines: simulations and measurements on the 230 kV Malta-Sicily Interconnector," Conference: CIGRE 2016, Paris, August 2016.

[39] A. Pagnetti, “Cable modelling for electromagnetic transients in power systems," Ph.D. dissertation, Université Blaise Pascal - Clermont-Ferrand II, 2012.

[40] D.Nasser Tleis Short-circuit analysis techniques in ac power systems December

---

Received: 30.04.22; **Similarities**: 18.05.22: **Reviewed**: 11.06./07.06.22: **Accepted**:20.06.22.

2008 DOI: 10.1016/B978-075068074-5.50010-2 In book: Power Systems Modeling and Fault Analysis

[41] C. DiBiasio Electromagnetic field emissions from underwater power cables Thesis Florida Atlantic University Boca Raton, Florida December 2014.

[42] W.Wang et al., "Failure of submarine cables used in high-voltage power transmission: Characteristics, mechanisms, key issues and prospects, " *IET Generation, Transmission & Distribution* , vol. 15, no. 9, pp. 1387-1402, 2021 https://doi.org/10.1049/gtd2.12117.

[43] S.J. Ryu, G.E Kim and B.W. Kim, "Conducted noise and transient voltage in a subsea cable" Proc IMechE Part M: J Engineering for the Maritime Environment, 2016, DOI: 10.1177/1475090215626461.

[44] N. Parmar, et al., "Switching Over Voltages in Offshore Cable Connections," ICRISET2017, 2017, Pages 586-592.

SIMULAREA CÂMPULUI MAGNETIC AL CABLULUI DE ALIMENTARE SUBMARIN CU TREI NUCLEE

Rezumat: Mai multe cercetări au fost efectuate cu privire la efectul electromagnetic în cablurile de alimentare submarine datorită interacțiunii magnetice a liniilor electrice asupra materialelor și mediului. Lucrarea noastră își propune să studieze simularea numerică bidimensională prin utilizarea metodei elementului finit al unui cablu de alimentare submarin cu trei nuclee. Rezultatele simulării ilustrează câmpul magnetic în condiții normale și anormale: sub suprasarcină și diferite forme de undă ale defecțiunilor curente ca funcții ale timpului și distanței, în trei faze. Rezultatele expun emisia de câmp magnetic a cablului electric submarin de înaltă tensiune, distribuția, forma de undă și intensitățile din jurul și din apropierea cablului subacvatic.

Wafa KRIKA PHD, Professor Hassiba Ben Bouali, University, Department of Mechanical engineering, Chlef, N19, Ouled Fares 02000, Algeria , Email: w.krika@univ-chlef.dz Phone: +213 661244622, Address: 14 zoubir ibn el aoueme Sidi Bel Abbes Algeria.

Ahmed Nour El Islam AYAD is an associate professor in Department of Electrical Engineering, Kasdi Merbah University, Ouargla 30000 Algeria, Email: ayad.ahmed@univ-ouargla.dz mailto:wafa2281988@hotmail.com Phone: +213 661244622, Address: 14 zoubir ibn el aoueme Sidi Bel Abbes Algeria.

Abdelghani AYAD is an associate professor in Department of Electrical Engineering, Djellali liabes University, sidi bel abbes 22000 Algeria Email: ayad_abdelghani@yahoo.fr Phone: +213667413956, Address: 56 Bab Daya Sidi Bel Abbes Algeria.